Available online at www.sciencedirect.com
SCIENCE DIRECT®
International Journal of Rock Mechanics & Mining Sciences 43 (2006) 203–215
International Journal of Rock Mechanics and Mining Sciences
www.elsevier.com/locate/ijrmms

Empirical estimation of rock mass modulus

E. Hoek[a,*], M.S. Diederichs[b]

[a]P.O. Box 75516, North Vancouver, British Columbia, Canada V7R 4X1
[b]Queen's University, Miller Hall, Kingston, Ont., Canada, K7L 3N6

Accepted 9 June 2005
Available online 15 August 2005

Abstract

The deformation modulus of a rock mass is an important input parameter in any analysis of rock mass behaviour that includes deformations. Field tests to determine this parameter directly are time consuming, expensive and the reliability of the results of these tests is sometimes questionable. Consequently, several authors have proposed empirical relationships for estimating the value of rock mass deformation modulus on the basis of classification schemes. These relationships are reviewed and their limitations are discussed. Based on data from a large number of in situ measurements from China and Taiwan a new relationship, based upon a sigmoid function, is proposed. The properties of the intact rock as well as the effects of disturbance due to blast damage and/or stress relaxation are also included in this new relationship.
© 2005 Elsevier Ltd. All rights reserved.

Keywords: Rock mass; Classification; Deformation modulus; In situ tests; Specimen damage; Blast damage; Disturbance

1. Introduction

The deformation modulus of a rock mass is an important input parameter in any analysis of rock mass behaviour that includes deformations. For example, in designing the primary support and final lining for a tunnel, the deformations of the rock mass surrounding the tunnel are important and a numerical analysis of these deformations requires an estimate of the rock mass deformation modulus. Field tests to determine this parameter directly are time consuming, expensive and the reliability of the results of these tests is sometimes questionable. Consequently, several authors have proposed empirical relationships for estimating the value of an isotropic rock mass deformation modulus on the basis of classification schemes such as the Rock Mass Rating (RMR) [1], the Tunnelling Quality Index (Q) [2] and the Geological Strength Index (GSI) [3].

Most authors have based their predictions on field test data reported by Serafim and Pereira [4] and Bieniawski [5] and, in some cases, by Stephens and Banks [6]. These data together with the most widely known equations are plotted in Fig. 1 and listed in Table 1. While most of these equations give reasonable fits to the field data, all of the exponential equations give poor estimates of the deformation modulus for massive rock because of the poorly defined asymptotes. Read et al. [7] attempted to limit the predicted rock mass modulus for massive rock by using a third power curve and this was also adopted by Barton [8]. The intact rock modulus (E_i) has been included in the equations proposed by Mitri [9], Sonmez et al. [10] and Carvalho [11] but these equations give relatively poor fits to the full range of data included in Fig. 1.

Some other authors have proposed equations relating rock mass modulus to other classification schemes such as RMi [15] and RQD [16] which are not readily accommodated in the discussion presented here. However, Zhang and Einstein's paper [16] is interesting in that, based on a paper by Kulhawy [17], they plot a family of curves showing the rate of increase in rock

*Corresponding author.
E-mail addresses: ehoek@attglobal.net (E. Hoek), mdiederi@geol.queensu.ca (M.S. Diederichs).

1365-1609/$ - see front matter © 2005 Elsevier Ltd. All rights reserved.
doi:10.1016/j.ijrmms.2005.06.005

mass modulus decreasing as joint spacing increases. The authors adopted similar reasoning when choosing a sigmoid equation to constrain the increase of modulus as the rock becomes more massive.

Note that all of the correlations discussed above as well as those presented in this paper assume that the rock mass is isotropic. Obviously there are situations, such as foundations on schistose rock masses, where the variation of modulus with loading direction is important. These conditions are outside the scope of this paper as are numerical model simulations of the modulus of discontinuous systems.

Before presenting an alternative equation the authors consider that it is necessary to review the in situ test methods and the interpretation of the results of in situ tests.

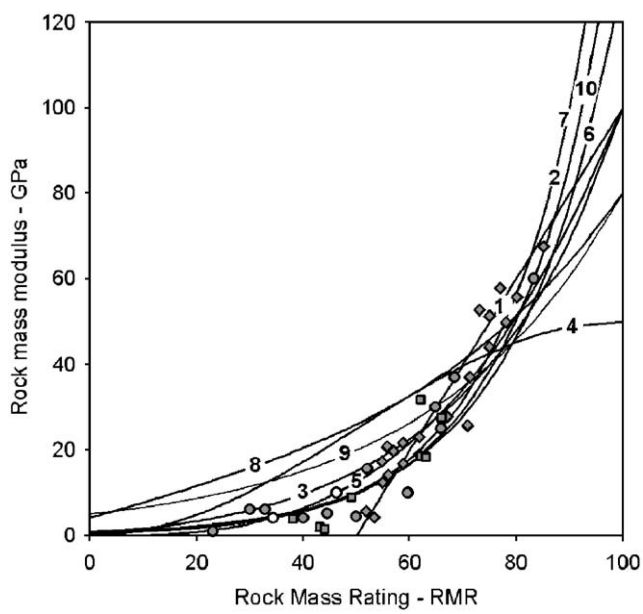

Fig. 1. Empirical equations for predicting rock mass deformation modulus compared with data from in situ measurements.

2. In situ test methods

The most common in situ test for the determination of the deformation modulus of a rock mass is the plate loading test or jacking test such as those shown in Figs. 2 and 3. These tests involve either a pressurized flat jack acting against a strut or a set of hydraulic jacks which apply the load to a prepared surface.

Measurement of the displacement of the loading plates, as is frequently done in these tests, results in significant inaccuracies. This is because of deflections of the plates, closure of gaps between the plates and the rock mass and closure of cracks in the blast damaged and stress relieved rock under the loading plates. This question has been examined in detail by Ribacchi [18] who concludes that reliable results can be obtained only when the displacements are measured at depth below the loading plates. Hence, where possible, deformations should be measured by means of a multi-point extensometer in the rock mass as shown in Fig. 2.

The interpretation of the measurements from such a test requires considerable care since, as shown in Fig. 4, there are several alternative definitions that can be applied to the deformability of the rock mass. The initial tangent modulus (1), related to the initial part of the stress–strain curve, is probably not related to the properties of the rock mass but is associated with the closing of gaps in the near surface rock and the mechanical components of the loading system.

Some authors quote both the elastic tangent modulus or modulus of elasticity (2) and the (secant) modulus of deformation (4). For an undamaged, confined rock mass, the two values should be similar. In practice, most authors quote only the modulus of deformation results which typically give low estimates for deformability of the rock mass.

An alternative method of in situ testing for rock mass modulus was devised by Dr. Manuel Rocha of the National Laboratory for Civil Engineering in Lisbon in

Table 1
Data and fitted equations for estimation of rock mass modulus plotted in Fig. 1

●	Field data	Serafim and Pereira [4]
◆	Field data	Bieniawski [5]
■	Field data	Stephens and Banks [6]
1	$E_{rm} = 2\mathrm{RMR} - 100$	Bieniawski [5]
2	$E_{rm} = 10^{((\mathrm{RMR}-10)/40)}$	Serafim and Pereira [4]
3	$E_{rm} = E_i/100(0.0028\mathrm{RMR}^2 + 0.9\exp(\mathrm{RMR}/22.82)), E_i = 50\,\mathrm{GPa}$	Nicholson and Bieniawski [12]
4	$E_{rm} = E_i(0.5(1-\cos(\pi\mathrm{RMR}/100))), \quad E_i = 50\,\mathrm{GPa}$	Mitri et al [9]
5	$E_{rm} = 0.1(\mathrm{RMR}/10)^3$	Read et al. [7]
6	$E_{rm} = 10Q_c^{1/3}$ where $Q_c = Q\sigma_{ci}/100,\ \sigma_{ci} = 100\,\mathrm{MPa}$	Barton [8]
7	$E_{rm} = (1-D/2)\sqrt{\sigma_{ci}/100} \times 10^{((\mathrm{RMR}-10)/40)}, \quad D = 0,\ \sigma_{ci} = 100\,\mathrm{MPa}$	Hoek et al. [13]
8	$E_{rm} = E_i(s^a)^{0.4},\ E_i = 50\,\mathrm{GPa},\ s = \exp((\mathrm{GSI}-100)/9),$ $a = 1/2 + 1/6(\exp(-\mathrm{GSI}/15) - \exp(-20/3)),\ \mathrm{GSI} = \mathrm{RMR}$	Sonmez et al. [10]
9	$E_{rm} = E_i s^{1/4},\ E_i = 50\,\mathrm{GPa},\ s = \exp((\mathrm{GSI}-100)/9)$	Carvalho [11]
10	$E_{rm} = 7(\pm 3)\sqrt{Q'}, \quad Q' = 10((\mathrm{RMR}-44)/21)$	Diederichs and Kaiser [14]

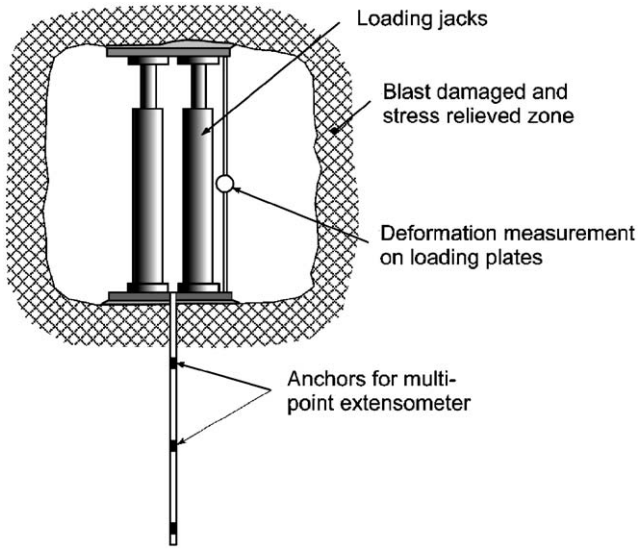

Fig. 2. Set-up for a plate jacking test with a multi-point extensometer installed in the rock mass and deformation measurement on the loading plates.

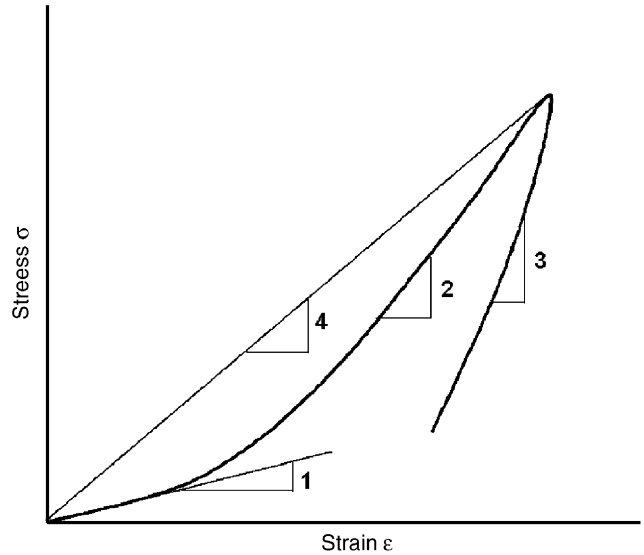

Fig. 4. Alternative definitions for the deformability of a rock mass. (1) Initial tangent modulus, (2) elastic tangent modulus, (3) recovery modulus and (4) modulus of deformation.

Fig. 3. In situ jacking test in an exploration adit for the New Tienlun hydroelectric project in Taiwan.

the 1960s [19] and this was used in several large dams in Portugal and its African territories. This method involved cutting a deep slot into the rock mass by means of a diamond impregnated saw as shown in Fig. 5. A large flat jack (Fig. 6) was then inserted into the slot and pressurized to induce deformations which were measured to determine the modulus of deformation. While this method gave reliable results, it was time consuming and expensive and it has not been used in recent years.

Large-scale tests using pressure chambers were proposed by Oberti et al. [20] in 1983 but these have only been used on a few projects because of the time and expense involved. Similarly, a detailed back analysis of deformation associated with an advancing tunnel face was reported by Tanimoto [21] but, as far as the authors are aware, only one such study was conducted. The details of this test are shown in Fig. 7 in which deformation measurements were made using a strain-gauged aluminium tube grouted into a borehole 2 m above and parallel to the axis of a 10 m span tunnel. A three-dimensional finite analysis of the deformation of the rock mass around the advancing tunnel face provided a curve which could be fitted to the measured deformations to obtain an estimate of the rock mass deformation modulus.

During the past decade, the availability of powerful numerical analysis codes has made it possible to back-analyse the behaviour of rock masses surrounding tunnels and to estimate or verify estimates of rock mass properties that give the best correlation between predicted and measured behaviour. The results of several such back analyses have been included in the database analysed by the authors in the next section of this paper. We anticipate that such back-analyses will become the most important source of reliable data in the future.

Fig. 5. Diamond impregnated saw for creating deep slots in a rock mass for flat jacks. Photographed by E. Hoek in LNEC laboratory, Lisbon, 1974.

Fig. 6. Flat jack for installation in the deep slot created by the saw shown in Fig. 5. Photographed by E. Hoek in LNEC laboratory, Lisbon, 1974.

The authors have found that the least reliable in situ measurements in this study are those from various down-hole jacks and borehole pressure meters. The measurements obtained from such devices are difficult to interpret, particularly in hard, jointed rock masses in which the stressed rock volume is obviously too small. The overall scatter in the data from these devices follow no logical patterns and it has been decided to remove this information from our database.

3. Description of new database

As part of this review of methods of estimating an isotropic rock mass modulus the authors were provided with a large database of in situ measurements by Dr. J.C. Chern of Taiwan. Details of this database, after removal of unreliable data such as those from borehole jacking tests, are presented in Table 2. This shows the number of tests for different rock types, different countries and different types of test.

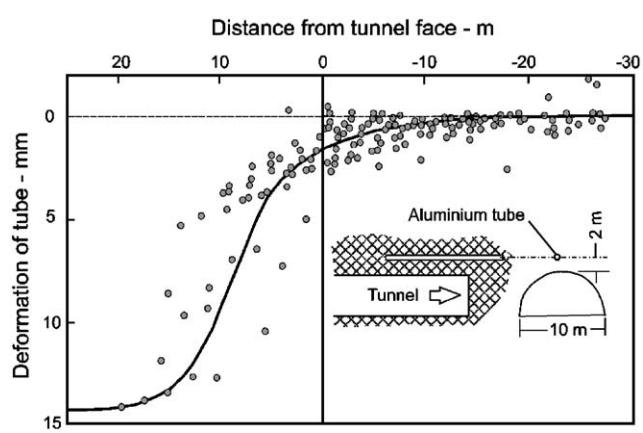

Fig. 7. Measurement of deformation of the rock mass surrounding an advancing tunnel face after Tanimoto [21].

The following relationships between the RMR and GSI, as suggested by Hoek and Brown [3], have been used in the analysis of this new data:

Pre-1990, $GSI = RMR_{76}$,
Post-1990, $GSI = RMR_{89} - 5$.

Table 2
Details of in situ tests in new database

Rocktype	Number of tests	Rocktype	Number of tests	Rocktype	Number of tests
Sedimentary	260	Igneous	179	Metamorphic	55
Sandstone	117	Basalt	46	Slate	26
Limestone	61	Migmatite	35	Quartzite	10
Siltstone	54	Aglomerate	30	Argillite	7
Silty-Shale	7	Diorite	20	Chlorite	2
Claystone	2	Granite	16	Gneiss	2
Conglomerate-Mudstone	6	Dolerite	15	Schist	2
Mudstone	5	Andesite	11	Metaconglomerate	6
Shale	5	Andesite-Tuff	5		
Sandy-Shale	3	Gabbro	1		
Year					
2000–2005	12				
1990–1999	197			*RMR or GSI ranges*	
1980–1989	141			0–20	4
1970–1979	126			20–30	22
1960–1969	18			30–40	42
				40–50	67
Country				50–60	96
China	457			60–70	163
Taiwan	37			70–80	63
				80–90	33
				90–100	4
Test Type					
Back Analysis	18				
Flat Jack	53				
Plate Tests	423				

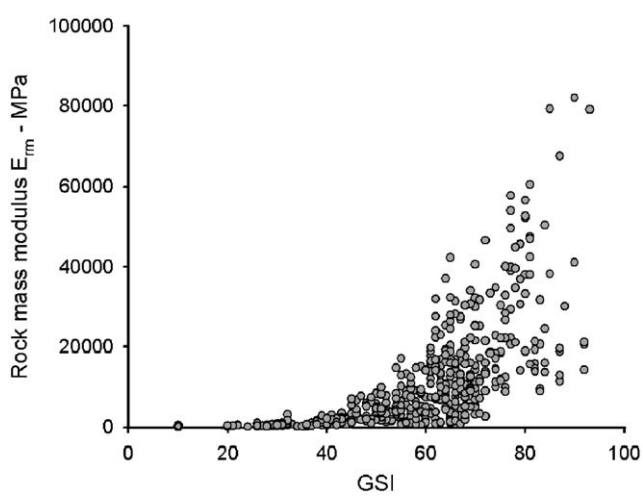

Fig. 8. Measured rock mass modulus of deformation against GSI for Chinese and Taiwanese data.

A plot of all the measured in situ deformation moduli against GSI from China and Taiwan is given in Fig. 8. Since most applications in which the modulus of deformation is required are in terms of stresses in MPa, it has been decided that all of this modulus data will be presented and analysed in terms of MPa rather than the more usual GPa units.

4. Simplified analysis of new data

In analysing the new data from China and Taiwan the authors have made the following assumptions:

1. This data set represents the best collection of quality field data which is likely to be available to any researcher. Scatter in the data represents inherent scatter in the values of GSI, intact rock properties, rock mass modulus E_m, and the effects of disturbance due to blasting and/or stress relief.
2. The upper bound of the data set represents the rock mass modulus of confined and undisturbed or undamaged rock such as that which would exist around a tunnel at depth.
3. The disturbance or damage that reduces the rock mass modulus from this upper bound can be represented by the disturbance factor D introduced by Hoek et al. [13]. A discussion on the factor D and guidelines for the choice of appropriate values for D are given in Section 7.
4. The maximum rock mass modulus corresponds to the deformation modulus of massive rock which is characterised by a GSI value of 90–100.
5. The modulus estimates discussed in this paper apply to isotropic rock masses.

6. In order to constrain the increase of modulus with increasing GSI, a sigmoid function is used as a basis for this analysis. This S shaped function has the following general form:

$$y = c + \frac{a}{1 + e^{-((x-x_0)/b)}}. \quad (1)$$

Based on these assumptions an analysis was carried out on the Chinese and Taiwanese data plotted in Fig. 8. Using commercial curve fitting software, Eq. (1) was fitted to these data and the constants a and b in the fitted equation were then replaced by expressions incorporating GSI and the disturbance factor D which were adjusted to give the equivalent average curve and the upper and lower bounds into which >90% of the data points fitted. Note that the constant $a = 100\,000$ in Eq. (2) is not directly related to the physical properties of the rock mass.

The following best-fit equation was derived:

$$E_{\mathrm{rm}}(\mathrm{MPa}) = 100,000\left(\frac{1 - D/2}{1 + e^{((75+25D-\mathrm{GSI})/11)}}\right). \quad (2)$$

A more detailed analysis will be presented in the next section and hence Eq. (2) will be called the Simplified Hoek and Diederichs equation.

Curves generated from Eq. (2) have been superimposed on the data points from China and Taiwan in Fig. 9. An average $D = 0.5$ (partially disturbed) was assumed for the overall analysis. The upper and lower bounds were defined by $D = 0$ (undisturbed) and $D = 1$ (fully disturbed), respectively.

In testing massive rocks with GSI values approaching 100, the deformations induced in the test are of the same order as the resolution of the measuring equipment. This gives rise to significant errors which show up as the outliers in Fig. 9. This problem can be overcome by averaging measurements from a single site, as has been done in Section 5. However, the authors decided to plot all of the data in Figs. 8 and 9 to show the range of values that can be anticipated in field tests.

The intact properties of the rock are not considered in the simplified relationship in Eq. (2). Eq. (2) is recommended when reliable property data for the intact rock is not available. The curve for $D = 0$ in this equation does, however, provide a reliable upper bound.

In order to independently test the adequacy of Eq. (2), it has been compared with the measured field data reported by Serafim and Pereira [4], Bieniawski [5] and Stephens and Banks [6]. These data are from high-quality tests and are generally considered reliable. All of these data were collected before 1989 and hence it has been assumed that $\mathrm{GSI} = \mathrm{RMR}_{76}$.

From Fig. 10 it can be seen that the Simplified Hoek and Diederichs Eq. (2) gives a good fit to this field data for $D = 0$ (upper bound, undisturbed conditions).

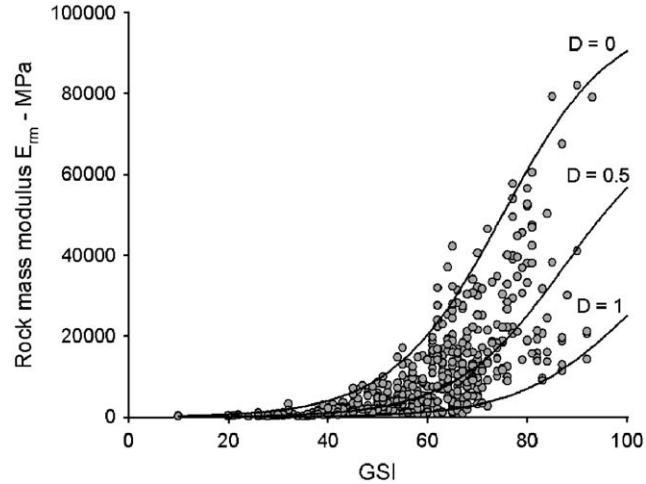

Fig. 9. Plot of Simplified Hoek and Diederichs equation for Chinese and Taiwanese data.

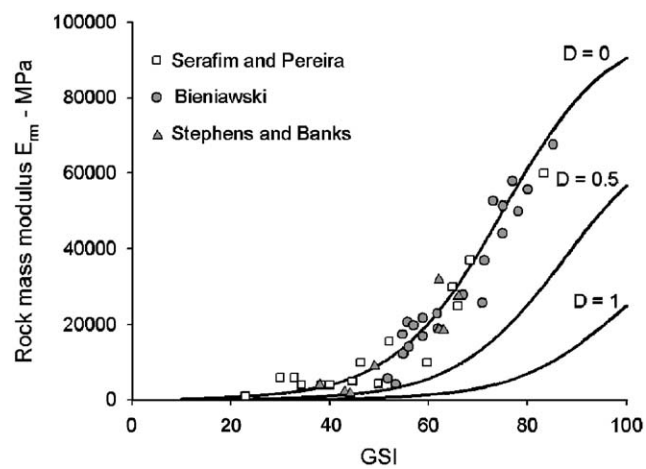

Fig. 10. Plot of in situ rock mass deformation modulus data from Serafim and Pereira [4], Bieniawski [5] and Stephens and Banks [6] against Simplified Hoek and Diederichs equation (2).

5. Detailed analysis of selected data

The rock mass deformation modulus data from China and Taiwan includes information on the geology as well as the uniaxial compressive strength of the intact rock (σ_{ci}). This information permits a more detailed analysis in which the ratio of mass to intact modulus ($E_{\mathrm{rm}}/E_{\mathrm{i}}$) can be included. Using the modulus ratio MR proposed by Deere [22] (modified by the authors based in part on this data set and also on additional correlations from Palmstrom and Singh [15]) it is possible to estimate the intact modulus from

$$E_{\mathrm{i}} = \mathrm{MR}\sigma_{\mathrm{ci}}. \quad (3)$$

This relationship is useful when no direct values of the intact modulus (E_{i}) are available or where completely undisturbed sampling for measurement of E_{i} is difficult.

A detailed analysis of the Chinese and Taiwanese data, using Eq. (3) to estimate E_i resulted in the following equation:

$$E_{rm} = E_i\left(0.02 + \frac{1 - D/2}{1 + e^{((60+15D-GSI)/11)}}\right). \quad (4)$$

This equation incorporates a finite value for the parameter c (Eq. (1)) to account for the modulus of fully broken rock (transported rock, aggregate or soil) described by GSI = 0. This equation is plotted against the average normalized field data from China and Taiwan in Fig. 11.

Table 3, based on the modulus reduction (MR) values proposed by Deere [22] can be used for calculating the intact rock modulus E_i. In general, measured values of E_i are seldom available and, even when they are, their reliability is suspect because of specimen damage. This specimen damage has a greater impact on modulus than on strength and, hence, the intact rock strength, when available, can usually be considered more reliable.

Data from Martin and Stimpson [23] show that severe sample damage (micro-cracking) due to stress relaxation, even in visibly intact rock (GSI = 100), can reduce the elastic modulus by up to 50% compared to undamaged samples and compared to geophysical determination of the confined modulus at depth. This observation is reflected in the limiting $D = 1$ curve for GSI = 100 in Eq. (4) and Fig. 11. This type of damage may also occur in a zone adjacent to excavations at depth well before any visible yield is observed. Similar grain scale damage can also be induced by excessive blasting.

Ribacchi [18] had reported measured in situ moduli up to twice the value for intact non-foliated rocks and even higher values for foliated rocks. He also suggests that micro-cracking due to stress relief is the most likely cause for these unusual results. It is particularly important to note the additional footnotes to Table 3 on the selection of MR values for foliated rocks.

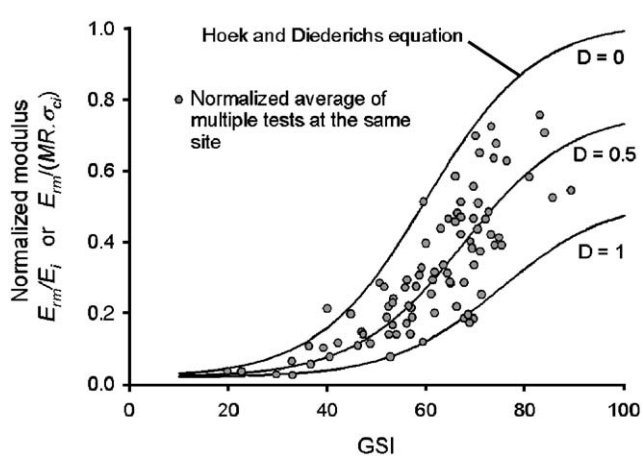

Fig. 11. Plot of normalized in situ rock mass deformation modulus from China and Taiwan against Hoek and Diederichs equation (4). Each data point represents the average of multiple tests at the same site in the same rock mass.

The relative effect of damage is greater for jointed rock masses (GSI < 80) as shown in Fig. 11. This is consistent with findings from Palmstrom and Singh [15] who found that, for GSI = 50–70, the measured moduli for TBM driven tunnels ($D = 0$) was 2–3 times higher than blasted tunnels ($D = 0.5-1$) for the same rock masses.

Using the product of the MR values listed in Table 3 and the values of σ_{ci} measured in the laboratory, the "intact" rock modulus values from Eq. (3) for the Chinese and Taiwanese data were calculated and substituted into Eq. (4) to produce the plot given in Fig. 12 (assuming $D = 0.5$). This compares the average measured and the calculated rock mass modulus plotted on a log scale to show the differences more clearly. This plot shows excellent agreement between the calculated values and the average measured values and suggests that Eq. (4) provides an estimate of rock mass modulus which is sufficiently accurate for most practical engineering applications.

6. Comparison between predictive models

A final check on the adequacy of the Hoek and Diederichs equations is carried out by comparing the errors involved in predicting the deformation modulus of individual in situ measurements as shown in Fig. 13. This comparison is based upon an error ratio, ER, for overestimated values and ER* for underestimated values defined as

$$ER = \frac{\text{Calculated } E_{rm}}{\text{Measured } E_{rm}},$$
$$ER^* = \frac{\text{Measured } E_{rm}}{\text{Calculated } E_{rm}}. \quad (5)$$

Using the Chinese and Taiwanese data set, this error ratio is plotted against GSI for the calculated rock mass moduli by Serafim and Pereira [4], Read et al. [7], Eqs. (2) and (4) in Fig. 14.

The improved accuracy of the Hoek and Diederichs equations is evident from this plot and it is also clear that, where information on the uniaxial compressive strength of the intact rock is available, the detailed Hoek and Diederichs solution in Eq. (4) should be used in conjunction with Eq. (3). If reliable intact modulus data is available then Eq. (4) may be used alone.

7. Guidelines for the disturbance factor *D*

The disturbance factor D was introduced by Hoek et al. [13] and there is not a great deal of experience on

Table 3
Guidelines for the selection of modulus ratio (MR) values in Eq. (3)—based on Deere [24] and Palmstrom and Singh [15]

Rock type	Class	Group	Texture			
			Coarse	Medium	Fine	Very fine
Sedimentary	Clastic		Conglomerates 300–400 Breccias 230–350	Sandstones 200–350	Siltstones 350–400 Greywackes 350	Claystones 200–300 Shales 150–250[a] Marls 150–200
	Non-clastic	Carbonates	Crystalline limestones 400–600	Sparitic limestones 600–800	Micritic Limestones 800–1000	Dolomites 350–500
		Evaporites		Gypsum (350)[b]	Anhydrite (350)[b]	
		Organic				Chalk 1000+
Metamorphic	Non-foliated		Marble 700–1000	Hornfels 400–700 Metasandstone 200–300	Quartzites 300–450	
	Slightly foliated		Migmatite 350–400	Amphibolites 400–500	Gneiss 300–750[a]	
	Foliated[a]			Schists 250–1100[a]	Phyllites/Mica Schist 300–800[a]	Slates 400–600[a]
Igneous	Plutonic	Light	Granite[c] 300–550 Granodiorite[c] 400–450	Diorite[c] 300–350		
		Dark	Gabbro 400–500 Norite 350–400	Dolerite 300–400		
	Hypabyssal		Porphyries (400)[b]		Diabase 300–350	Peridotite 250–300
	Volcanic	Lava		Rhyolite 300–500 Andesite 300–500	Dacite 350–450 Basalt 250–450	
		Pyroclastic	Agglomerate 400–600	Volcanic breccia (500)[b]	Tuff 200–400	

[a]Highly anisotropic rocks: the value of MR will be significantly different if normal strain and/or loading occurs parallel (high MR) or perpendicular (low MR) to a weakness plane. Uniaxial test loading direction should be equivalent to field application.
[b]No data available, estimated on the basis of geological logic.
[c]Felsic Granitoids: coarse grained or altered (high MR), fined grained (low MR).

its use. From the results presented in the preceding discussion it is clear that it has a significant influence upon the estimated rock mass modulus of deformation and this influence appears to be in accordance with practical observations and engineering reasoning.

The disturbance of the rock mass will vary with distance from a free face due to blast damage and stress relief and, in some cases, to stress induced fracturing. In a recent tunnel design project the authors assumed that the value of D varied in proportion to the strain induced in the failure zone surrounding the tunnel. Very few numerical models allow this variation to be incorporated directly into the model but it is generally possible to include a number of concentric rings around the

excavation and to assign a lower value of D to each successive ring. This procedure can be used for either the back analysis of measured deformations in order to estimate the deformation modulus or a design in which estimated deformation modulus values are applied in order to calculate the deformations around the excavation.

It is difficult to give precise guidelines on the use of the disturbance factor D since this use will vary for each application, depending upon the excavation and loading sequence for the particular structure being designed. For example, the excavation and loading sequence for a foundation is quite different from that of a tunnel and the designer has to take these differences into account in

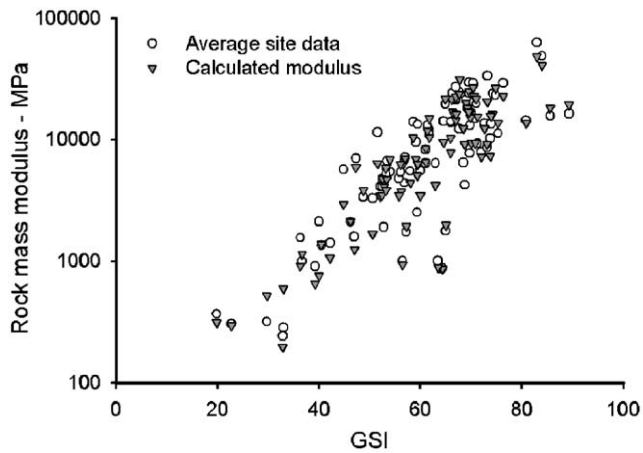

Fig. 12. Comparison between average measured rock mass deformation modulus (each point is the average of multiple tests at the same site in the same rockmass) from China and Taiwan with values calculated using Eq. (4) with average $D = 0.5$.

Fig. 14. Road cut in which the size of individual rock blocks is of the same order as the height of the cut. Rock mass classifications, based on the assumption of homogeneity, cannot be applied to this rock mass.

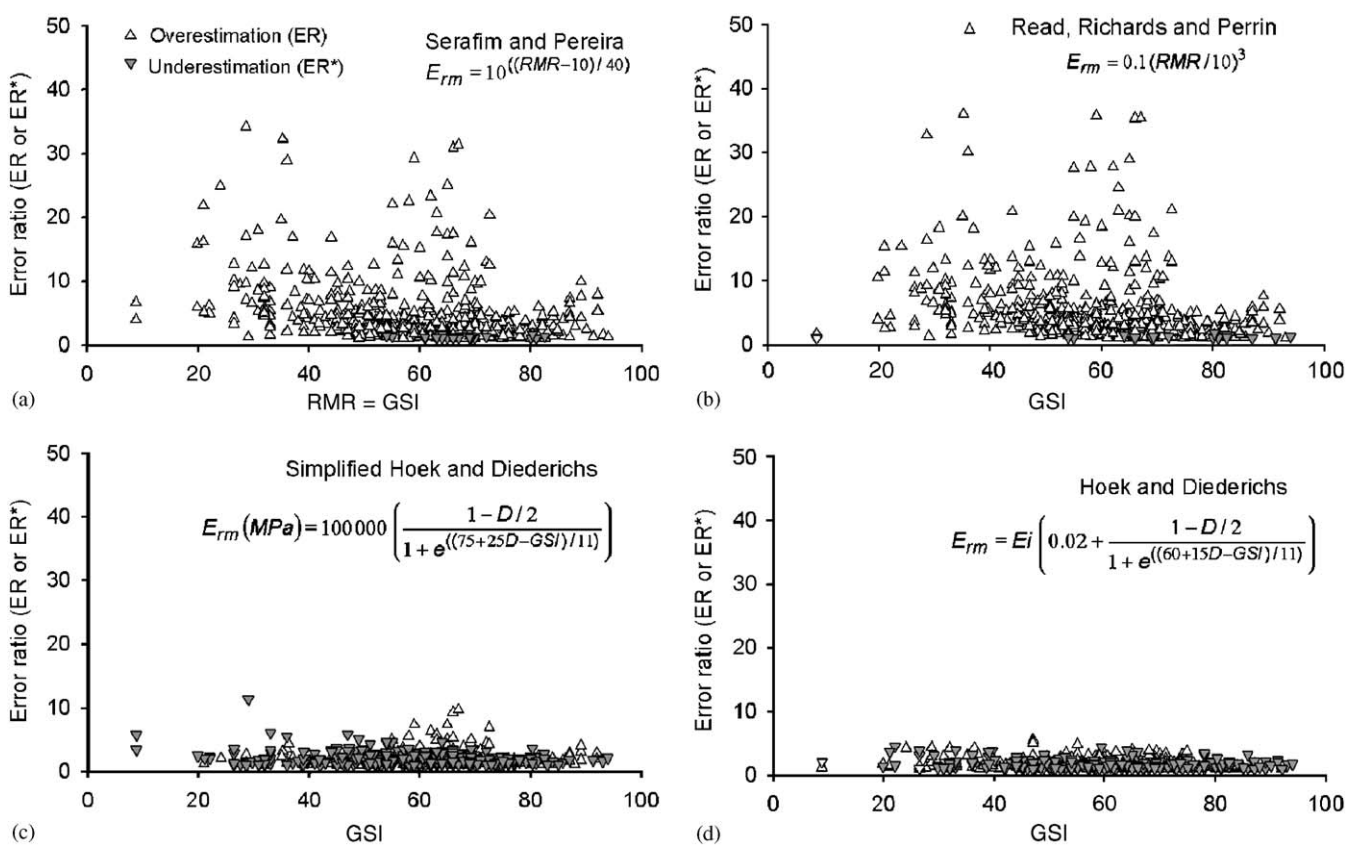

Fig. 13. Comparison of prediction errors ($D = 0.5$ for Hoek and Diederichs).

formulating the approach to be used in each case. Hence, rather than attempt to present a table of recommended D values the authors have chosen to present a number of case histories which illustrate how the disturbance factor was incorporated into each analysis. It is hoped that these case histories will provide the reader with sufficient guidance to choose an appropriate range of disturbance factors for their own applications.

It is also important to point out that the results of numerical analyses have to be treated with great care in rock engineering design applications. The inherent variability of all of the input data will always give a significant level of uncertainty, in spite of the sophistication and precision of the numerical methods available today. Hence, it is always important that a designer who uses these numerical tools should not be tempted to accept the results from a single analysis but rather should carry out a set of parametric studies in which each input parameter is varied over a range of credible values in order to obtain an understanding of the sensitivity of the design to these variations. In fact the sensitivity of a design to changes in the input parameters is probably more important in judging the acceptability of the design than any single calculated deformation value or factor of safety.

An important issue that requires clarification before discussing the details of the factor D is that of the general use of rock mass classifications. All of these classifications are based on the assumption of isotropy and homogeneity. This means that a rock mass must contain a sufficient number of discontinuities sets so that its deformational behaviour can be considered isotropic.

The question of scale is an important factor here in that the size of the blocks in the 5 m high rock slope illustrated in Fig. 14 are such that this slope cannot be treated as a homogeneous mass. Hence the typical rock mass classifications are not applicable to this slope and its stability and deformational behaviour must be analysed on the basis of the three-dimensional geometry of the individual blocks. On the other hand, the same sized blocks in a large excavated open pit mine slope, such as that shown in Fig. 15, would result in nearly isotropic conditions and the rock mass, on this scale, would qualify as a homogeneous mass to which rock mass classifications could be applied.

Fig. 15 shows the excavated slopes in the Chuquicamta open pit mine in Chile and, as discussed above, the rock masses forming these slopes are treated as homogeneous and rock mass classification systems are used in estimating strength and deformation properties for analysis. These slopes are excavated by very large-scale production blasts and experience has shown that the zone of blast damaged and stress relieved rock can extend for 100 m or more behind the crest of the slope.

Fig. 15. Excavated slopes in the Chuquicamata open pit mine in Chile. These slopes are 850 m high and individual rock mass units are treated as homogeneous.

In analysing the stability of this loosened rock mass it is necessary to assign a disturbance factor $D \sim 1$ in using the Hoek–Brown failure criterion [13] to estimate rock mass properties relevant for slope stability.

Fig. 16 shows a surface outcrop of jointed sandstone on the site of the Mingtan Pumped Storage Project in Taiwan. Fig. 17 shows the results achieved by blasting the roof of a 22 m span powerhouse cavern in this rock mass. In spite of every effort to control blast damage, the inclined discontinuity surfaces in the rock mass resulted in an irregular excavation profile. Back analysis of the results of careful deformation measurements from extensometers installed from the cavern [24] showed that the damage and stress relaxation extended from 1.5 to 2 m behind the excavated faces. Hence, in analysing the overall cavern deformation, a disturbed zone (with $D = 0.5$) of approximately 2 m thick was "wrapped" around each excavation stage. The rock mass behind this zone was treated as undisturbed with $D = 0$.

Undisturbed rock mass conditions achieved by smooth blasting in massive gneiss in the underground powerhouse cavern of the Rio Grande Pumped Storage Project near Cordoba in Argentina are shown in Fig. 18. This 25 m span cavern required minimal support as a result of the quality of the blasting. In this case it would be appropriate to assign a disturbance factor $D = 0$ to the rock mass surrounding the cavern and to ignore any blast damaged or disturbed zone in design calculations.

Fig. 19 shows an exposure of folded sedimentary rocks in a carefully excavated road cutting in the vicinity of the Acheloos tunnel in Greece. In this case some disturbance of the rock mass is evident but it is considered to be relatively shallow. For design purposes

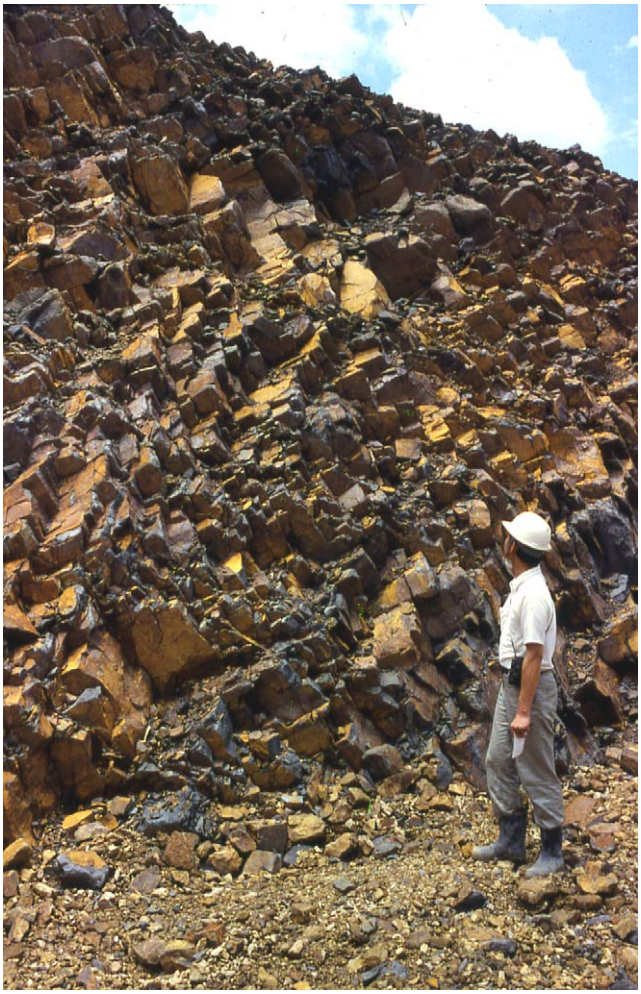

Fig. 16. Surface exposure of jointed sandstone on the site of the Mingtan Pumped Storage Project in Taiwan.

Fig. 17. Cavern profile achieved by drill and blast excavation in jointed sandstone.

it is suggested that a disturbance factor of $D = 0.3$ should be assigned to this rock mass.

On the other hand, in a similar rock mass close to the exposure illustrated in Fig. 19, undisturbed rock mass

Fig. 18. Undisturbed conditions achieved by smooth blasting in massive gneiss in the underground powerhouse cavern of the Rio Grande Pumped Storage Project in Argentina.

Fig. 19. Exposure of folded sedimentary rocks in a carefully excavated road cutting in the vicinity of the Acheloos tunnel in Greece.

Fig. 20. Undisturbed conditions achieved by TBM excavation in folded sedimentary rocks in the Acheloos tunnel in Greece.

conditions with $D = 0$ are shown in Fig. 20 in the wall of the TBM excavated Acheloos tunnel. This rock mass comprises interbedded sedimentary rocks which have been tightly folded by the tectonic actions associated with the formation of the Pindos mountain chain. These foliated rocks would be susceptible to problems of laboratory testing to determine the intact modulus. Hence, estimation of the overall rock mass modulus should be made on the basis of the GSI rating, according to Eq. (2), or from estimates of MR and the intact strength σ_{ci}, substituted into Eqs. (3) and (4).

8. Conclusions

An analysis of in situ rock mass modulus measurements for a wide range of rock types from China and Taiwan has resulted in two new equations for estimating rock mass deformation modulus. The upper bound values predicted by these equations fit historical measurements from several countries and it is concluded that these equations are universally applicable isotropic rock masses. It is recommended that these upper bound values be used for tunnel design where confined conditions exist. For shallow tunnels, slopes and foundations, the effects of rock mass disturbance can be taken into account by means of the disturbance factor D.

The simplified Hoek and Diederichs equation (2) can be used where only GSI (or RMR or Q) data are available. The more detailed Hoek and Diederichs equation (4) can be used where reliable estimates of the intact rock modulus or intact rock strength are available.

Acknowledgements

The generosity of Dr. J.C. Chern of Sinotech Engineering Consultant Inc, Taiwan who provided access to his databases on rock mass deformation modulus measurements in China and Taiwan is gratefully acknowledged. We are also grateful for the constructive comments provided by Dr. J.C. Chern of Taiwan, Dr. Jose Carvalho and Dr. Trevor Carter of Golder Associates of Toronto, Canada, Professor Derek Martin of the University of Alberta, Canada, Professor Renato Ribacchi of the University of Rome, Italy, Professor Harun Sonmez of Hacettepe University, Turkey, Dr. Brent Corkum of RocScience, Toronto, Canada, Dr. Carlos Carranza-Torres of Itasca, USA, Professor Z.T. Bieniawski of Arizona, USA and Dr. Laurie Richards, an independent consultant in New Zealand.

References

[1] Bieniawski ZT. Engineering classification of rock masses. Trans S African Inst Civ Engrs 1973;15(12):335–44.
[2] Barton N, Lien R, Lunde J. Engineering classification of rockmasses for the design of tunnel support. Rock Mech 1974;6(4):189–236.
[3] Hoek E, Brown ET. Practical estimates of rock mass strength. Int J Rock Mech Min Sci 1997;34(8):1165–86.
[4] Serafim JL, Pereira JP. Consideration of the geomechanical classification of Bieniawski. Proc. Int. Symp. Eng Geol Underground Construction (Lisbon) 1983;1(II):33–44.
[5] Bieniawski ZT. Determining rock mass deformability—experience from case histories. Int J Rock Mech Min Sci Geomech Abstr 1978;15.
[6] Stephens RE, Banks DC. Moduli for deformation studies of the foundation and abutments of the Portugues Dam—Puerto Rico. In: Rock mechanics as a guide for efficient utilization of natural resources: Proceedings of the 30th US symposium, Morgantown. Rotterdam: Balkema; 1989. p. 31–8.
[7] Read SAL, Richards LR, Perrin ND. Applicability of the Hoek–Brown failure criterion to New Zealand greywacke rocks. In: Vouille G, Berest P, editors. Proceedings of the nineth international congress on rock mechanics, Paris, August, vol. 2; 1999. p. 655–60.
[8] Barton N. Some new Q value correlations to assist in site characterisation and tunnel design. Int J Rock Mech Min Sci 2002;39:185–216.
[9] Mitri HS, Edrissi R, Henning J. Finite element modeling of cablebolted stopes in hard rock ground mines. Presented at the SME annual meeting, New Mexico, Albuquerque, 1994. p. 94–116.
[10] Sonmez H, Gokceoglu C, Ulusay R. Indirect determination of the modulus of deformation of rock masses based on the GSI system. Int J Rock Mech Min Sci 2004;1:849–57.
[11] Carvalho J. Estimation of rock mass modulus. Personal communication 2004.
[12] Nicholson GA, Bieniawski ZT. A nonlinear deformation modulus based on rock mass classification. Int J Min Geol Eng 1990;8:181–202.
[13] Hoek E, Carranza-Torres CT, Corkum B. Hoek-Brown failure criterion-2002 edition. In: Proceedings of the fifth North American rock mechanics symposium, Toronto, Canada, vol. 1, 2002. p. 267–73.
[14] Diederichs MS, Kaiser PK. Stability of large excavations in laminated hard rockmasses: the Voussoir analogue revisited. Int J Rock Mech Min Sci 1999;36:97–117.
[15] Palmstrom A, Singh R. The deformation modulus of rock masses: comparisons between in situ tests and indirect estimates. Tunnelling Underground Space Technol 2001;16:115–31.
[16] Zhang L, Einstein HH. Using RQD to estimate the deformation modulus of rock masses. Int J Rock Mech Min Sci 2004;41: 337–41.
[17] Kulhawy FH. Geomechanical model for rock foundation settlement. J Geotech Eng ASCE 1978;104:211–27.
[18] Ribacchi R. Rock mass deformability; in situ tests, their interpretation and typical results in Italy. In: Sakurai, editor. Proceedings of the second international symposium on field measurements in geomechanics. Balkema: Rotterdam; 1988.
[19] Rocha M, Da Silva JN. A new method for the determination of deformability of rock masses. In: Proceedings of the second congress on rock mechanics. Paper 2–21. International Society for Rock Mechanics, Belgrade, 1970.
[20] Oberti G, Coffi L, Rossi PP. Study of stratified rock masses by means of large scale tests with an hydraulic pressure chamber. In: Proceedings of the fifth ISRM congress, Melbourne, 1983. p. A133–41.

[21] Tanimoto C. Contribution to discussion in proceedings of the paris conference on analysis of tunnel stability by the convergence–confinement method (Published in Underground Space 4 (4)). Oxford: Pergamon Press; 1980.
[22] Deere DU. Chapter 1: geological considerations. In: Stagg KG, Zienkiewicz OC, editors. Rock mechanics in engineering practice. London: Wiley; 1968. p. 1–20.
[23] Martin DM, Stimpson B. The effect of sample disturbance on laboratory properties of Lac du Bonnet granite. Can Geotechn J 1994;31(5):692–702.
[24] Cheng Y, Liu SC. Power caverns of the Mingtan Pumped Storage Project, Taiwan. In: Hudson JA, editor. Comprehensive rock engineering, vol. 5; 1990. p. 111–32.